RESILIENT INFRASTRUCTURE
June 1–4, 2016
RESILIENT INFRASTRUCTURE LONDON 2016

BOND BEHAVIOUR OF GROUTED CONNECTIONS UNDER MONOTONIC TENSILE LOADS

Mohamed, Elsayed
PhD Student, University of Western Ontario, Canada

Douglas, James Provost-Smith
MSc Student, University of Western Ontario, Canada

Nehdi, Moncef
Professor, University of Western Ontario, Canada

Eissa, Osama
Principal, IES Associates, Canada

ABSTRACT

Grouted bar-in-conduit connections are versatile connections widely used in the precast concrete construction. In precast load bearing wall structures, two vertical wall panels are connected by a reinforcing bar, which is projected from one panel and grouted into a sleeve placed in the other. The main function of the ties is to resist tension induced by in-plane and out-of-plane straining actions and to provide ductility to the wall assembly through the yielding of the reinforcement. Limited information is currently available on the behaviour of such connections. This paper presents the findings of an investigation conducted to investigate the behaviour of grouted reinforcing bar connections and their failure mechanisms. The bond strength was evaluated using a pull-out test on a bar extended from a grouted sleeve specimen. The test parameters of the study were the bar surface condition (deformed and smooth) and the embedded length (6, 12 and 36 diameter-of-bar (d_b)). A total of eight specimens were tested to failure under direct tensile loads and the slip of the bars was recorded. Results indicate that an embedment length of $6d_b$ allowed the bar to yield, but bond failure dominated in the strain hardening zone. It was also observed that an embedment length of $12d_b$ was sufficient to mobilize the tensile capacity of the bar, after which an increase in the grouted sleeve length resulted in no additional capacity.

Keywords: Bond Strength, Precast Walls, Pull-out Tests, Grouted Connections

1. INTRODUCTION

In precast concrete systems, a grouted bar-in-conduit connection consists of a reinforcing bar projected from one element and grouted into a sleeve placed in the other. The scheme is used to transfer tension, compression or shear. This connection has applications in connecting a variety of precast concrete components, such as column-foundation, column-column, and wall-to-wall connections (PCI 2010). This type of connection is popular in precast load bearing construction, where it serves two main functions: tie the panels down against uplifting moments from lateral loads; and to serve as a ductile device that can yield in tension (CPCI 2007). The connection typically consists of a grouted steel duct that is used to house a continuous reinforcing bar from the foundation to the top of the wall as shown in Figure 1. Segments of the bar are connected using a coupler or by lap splicing. The spliced length sits in a grouted sleeve. A variety of different schemes exist for this connection, where the choice of the connection is dependent on the preference of the designer and fabricator since such connections are primarily based on previous construction practices.

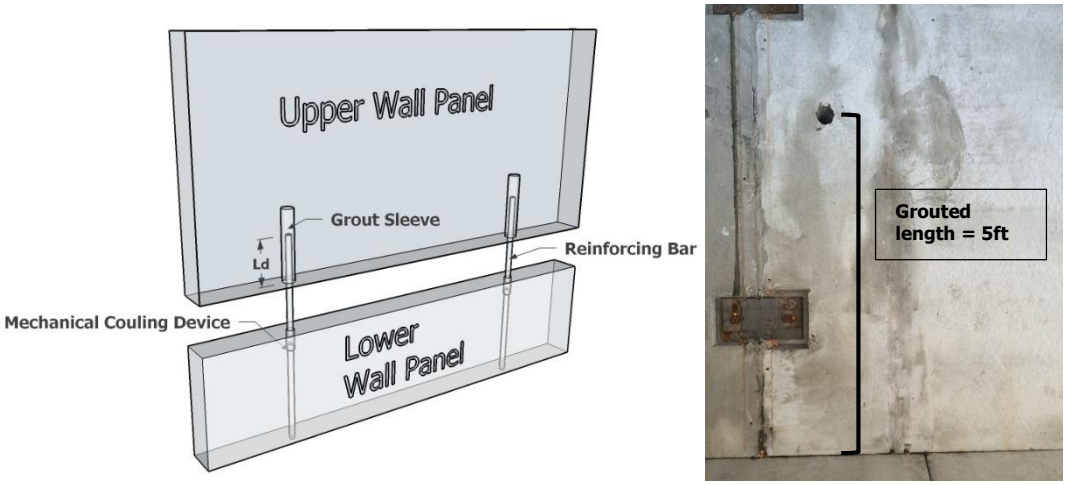

Figure 1: Illustration of (a) grouted reinforcing bar connection, and (b) grouted bar in conduit connection in shear walls of residential building (obtained with permission from Stubbe's Precast)

When lateral loads push a panel in the in-plane direction, some of the connections are exposed to tensile loads. If strain the bar is stressed beyond it's elastic limit, the bar yields and its post-yield deformation capacity provides ductility, which is often in the form of a horizontal gap opening between two vertically stacked panels. To be able to deliver this ductility to the assembly, the reinforcing bar should be well developed in the wall panel so that any brittle failure (slippage of the bar) is avoided. The development length of the bar in this case is the length of the grouted sleeve projected in the wall. Typical development length/bond models do not accurately depict the behaviour of these connections due to the presence of the sleeve and its consequent confinement effect. This paper presents the results of a series of tests carried out to quantify the behaviour of grouted reinforcing bar connections.

2. BACKGROUND

Precast concrete wall systems are designed to emulate cast in-situ concrete structures. Since cast-in-place walls are continuous, they resist lateral loads as a single monolithic unit. Because of their jointed nature, precast construction has inherent horizontal and vertical joints. Damage is highly concentrated in the joint regions, where planes of reduced stiffness can be introduced, creating dis-continuities in the structural framework of large panel precast construction (Fintel 1977). Thus, to achieve a comparable performance to that of conventional reinforced concrete, continuity across all joints is required. Recognizing the redundancies inherent to this structural discontinuity, most of the relevant design codes (e.g. ACI 318-14, PCI 7th Edition, CPCI 4) specify integrity clauses for the way elements are connected. The intent of the integrity clauses is to improve the ductility of structures by reducing the risk of failure or collapse resulting from localized damage to an element. Section 16.2.5 in ACI 318-14 state that a minimum of two ties per panel, each having a tensile capacity of 10 kips (44 kN), are to be provided. For large panel construction (panels having a horizontal dimension greater than their height), three or more stories high, a nominal tensile force of 3000 lb/ft (43.8 kN/m) per length of wall, is to be carried by at least two ties. The ties should be continuous from the top of the wall to the foundation(ACI Committee 318, 2014).

The PCI Design Handbook provides governing design and construction specifications of grout-filled metallic conduit connections. It specifies a minimum concrete cover of 3 in (76.2 mm); a minimum duct thickness of 0.023 in (0.6 mm); 0.375 in (9.5 mm) of minimum clearance around the bar; and a grout compressive strength of no less than 5000 psi (~35 MPa) (PCI 2010). Typically, a large diameter bar (20-30 mm) is used in a grout-filled bar connection depending on the size of the wall and its lateral loads. The minimum specified development length of a No. 8 bar (25 mm) is 42 in (1067 mm) for 5000 psi (35 MPa) concrete and the minimum embedment length of any bar should not be less than 12 in (305 mm) (ACI Committee 318, 2014; PCI 2010). Equation 1, which is used to calculate the latter development length, is the model adopted by ACI 318-14 based on the efforts of Orangun et al. and Darwin et al., where the length of a grouted sleeve connection is idealized as a bar embedded in concrete (ACI Committee 408, 2003).

[1] $$L_d = \left(\frac{3}{40} \frac{f_y}{\sqrt{f_c'}} \frac{\psi_t \psi_e \psi_s}{\left(\frac{c_b + k_{tr}}{d_b} \right)} \right) d_b$$

Where L_d = development length; f_y = yield strength of bar; $f_{c'}$ = concrete compressive strength; $\psi_t \psi_e \psi$ = factors accounting for bar casting position, bar coating and size, respectively; d_b = diameter of bar; K_{tr} = transverse reinforcement index and C_b = smaller of: (a) the distance from centre of a bar or wire to nearest concrete surface, and (b) one-half the centre-to-centre spacing of bars or wires being developed.
The bond of reinforcing bars in concrete has been widely investigated and substantial studies have been directed to exploring the bond behaviour, (e.g. Harajli et al. 2002; Tastani & Pantazopoulou 2010; Saleem et al. 2012; Dancygier et al. 2010). The embedment length of reinforcing bars in concrete is dependent on a number of factors, including the concrete strength (the ultimate bond strength is proportional to the square root of the compressive strength (Soroushian et al. 1991)); confinement effect (lateral pressure reduces the required length to develop a reinforcing bar (Ling et al. 2012; Ling et al. 2014; Hosseini et al. 2015)); reinforcing bar strength and roughness (higher strength reinforcement bars require longer development length to ensure full mobilization of the bar capacity (Saleem et al. 2012)).

Raynor et al. (2002) studied the bond-slip behaviour of grouted bar connections through a series of pull-out tests for small diameter bars. They concluded that grouted bar-in-duct connections behave differently than bars embedded in concrete due to the confining effect of the duct. Moreover, they found that higher bond stresses are attainable over a much shorter development length, making it possible to reduce the length of the connections. However, their research was designed to validate a constitutive model using 2 in (50.8 mm) development length without studying the behaviour of specimens with full development length. Moreover, Steuck et al. (2009) studied the anchorage requirements of large diameter bars (No.'s 10, 14 and 18 bars) used in precast bridge bent cap construction. The results were compared to the development length requirements of AASHTO and ACI. It was concluded that an embedment length of 10 d_b was sufficient to cause the bar to fracture. The test specimen utilized in his study was different, where one concrete block with a central duct was re-used for a number of tests. Therefore, the information provided by this study cannot be directly extrapolated to the applications of the grouted connections in precast load bearing walls.

The efficacy of using Equation 1 in calculating the length of a grouted bar connection is questionable since the additional confinement effect of the sleeve is not captured in this model. As a result, field grouting applications involve excessive lengths, sometimes exceeding 3ft (1.5 m) as shown in Figure 1(b). There is a clear need for a comprehensive study to: 1) investigate the bond behaviour of grouted reinforcing bar connections; and 2) test the performance and capacity of the connections used in the field to confirm the applicability of using the model adopted by ACI 318-14 in precast applications.

3. TEST SPECIMEN AND SETUP

The test configuration and specimen used to evaluate the bond strength of grouted reinforcing bar connections is depicted in Figure 2. A series of pull-out tests were carried out on specimen's representative of real field conditions. A non-reinforced concrete block was cast to represent the portion of a wall with a grouted sleeve connection, where a 3 in (76.2 mm) corrugated (hollow) sleeve was embedded. The cross-section of the specimen was 8 x 8 in (203 x 203 mm), similar to typical precast load bearing walls. The specimen height was 16 in (406 mm). The 6 and 12 d_b specimens where de-bonded over a length of 10 in (254 mm) and 4 in (101.6 mm), respectively. The reinforcing bar was extended above and below the concrete block by 1 in (25.4 mm) and 24 in (610 mm), respectively, to allow for a comfortable distance to grip the bar as well as sufficient clearance to observe fracture. The concrete and grout used to cast the specimens had a 28-day average compressive strength (obtained from two identical 4 x 8 in cylinders) of 7335 psi (50.61 MPa) and 5800 psi (40 MPa), respectively. The smooth steel and reinforcing bar used were both Grade 400 R mild steel rebar with a specified minimum yield strength of 400 MPa. The concrete specimens were grouted and cured in room temperature (approximately 23°C) for 28 days.

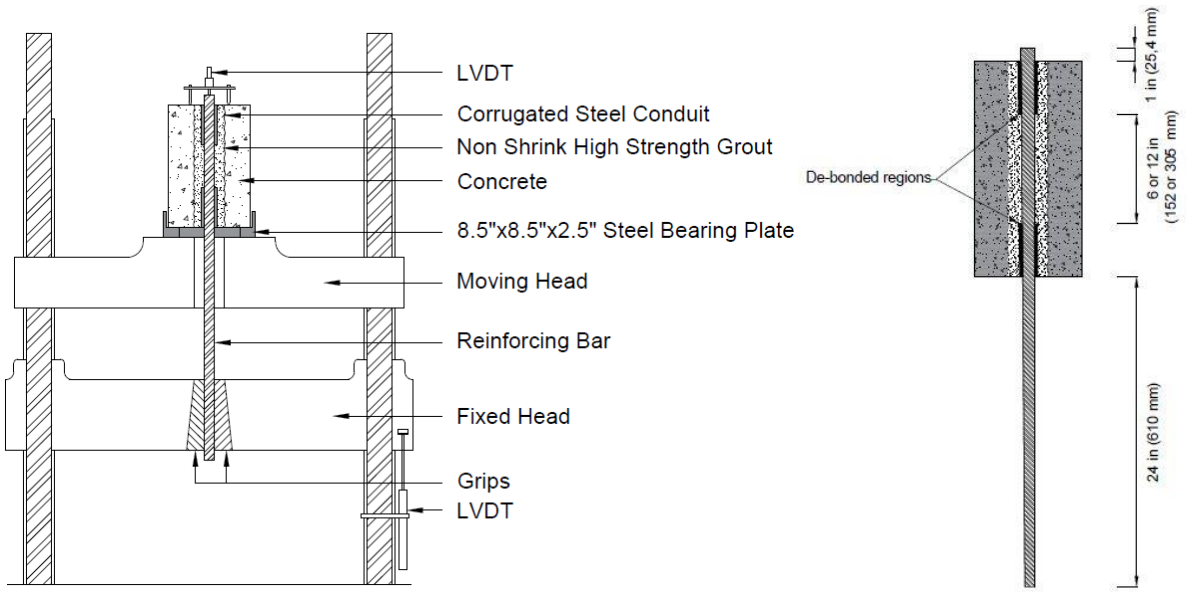

(a) (b)

Figure 2: (a) Pull-out test rig; (b) Specimen dimensions

To cast the specimen in the vertical position, a hollow steel table with a recessed ledge running along its perimeter was used to support four 4 x 4 in (102 x 102 mm) wood studs. The studs were spaced 10 in (254 mm) on centre, creating channels running across. Specimens were placed atop an 8 x 8 in (203 x 203 mm) wooden plate placed on the wooden studs. The reinforcing bar was extended through a 1 in (25.4 mm) hole punched through the wooden plate and propped 16 in (406 mm) above the floor. The non-shrink grout was mixed at low speed for 10 minutes and at high speed for 5 more minutes, continuously adding water until a self-levelling consistency was achieved. This grout mixing approach mimics field practice with similar commercial grouts. The grout was then poured and cured at the ambient temperature (approximately 23°C) of the lab for 28 days until testing. Figure 3b exhibits the setup used for casting.

The specimens were intentionally un-reinforced to reduce additional confinement that may be present due to typical wall reinforcements around the sleeve, which might result in an un-realistic estimate of the bond strength. Furthermore, an 8.5 x 8.5 x 2.5 in (216 x 216 x 63.5 mm) hollow steel bearing plate was placed between the specimen and the testing machine to reduce the effects of the confinement induced from the bearing of the specimens on the testing machine. Figure 3b shows de-bonded bars prior to casting. The top and bottom segments of the bar were de-bonded (using a 14 gauge (2 mm) thick polystyrene wrap to act as a bond breaker) to mitigate the additional confinement inherent from pull-out tests (Achillides & Pilakoutas 2004). The testing was done with an open loop Tinius Olsen machine with a 530 kN capacity. A 25 mm strain based linear variable displacement transducer (LVDT) was mounted by a steel tripod and was placed on the protruding bar from the top (unloaded end) to record the slip relative to the top surface of the specimen. The displacement at the loaded end of the specimen was monitored by measuring the relative displacement between the fixed and moving heads of the machine by a 150 mm spring LVDT. The measurements were recorded at a rate of 1 reading per second. The load was applied in load control at a monotonic rate of 60 MPa/min until failure. Figure 3c shows a specimen undergoing a test.

Figure 3: (a) Polystyrene bond breakers for the $6d_b$ bars; (b) Casting rig; and (c) Photograph showing the test setup

4. TEST RESULTS AND DISCUSSION

Table 1: Bond test results of smooth and deformed bars

[(1)]Specimen Tag	P_y (kN)	S_y (mm)	P_u (kN)	S_u (mm)	Δ_y (mm)	Δ_u (mm)	U_{max} (MPa)	S_{max} (mm)	f_{bu} (MPa)	R_y (P_y/P_y)	Failure Type
NS-6-S1	37.60	0.137	62.70	11.060	5.92	17.37	5.23	10.910	127.73	0.19	Pull-out
NS-6-S2	42.20	0.036	61.40	13.320	5.86	19.81	5.12	13.320	125.08	0.21	Pull-out
NS-6-D1	198.00	0.121	250.80	0.920	16.34	54.68	20.95	0.890	510.92	0.99	Pull-out
NS-6-D2	197.20	0.117	243.60	0.980	14.43	43.65	20.35	0.930	496.25	0.99	Pull-out
NS-12-S1	91.90	0.039	91.90	14.480	3.75	19.39	3.83	14.440	187.21	0.46	Pull-out
NS-12-S2	104.10	0.011	118.20	6.950	10.52	17.90	4.93	6.950	240.79	0.52	Pull-out
NS-12-D1	197.10	0.023	273.10	0.054	12.78	108.27	11.40	0.054	556.35	0.99	Bar Fracture
NS-12-D2	197.40	0.018	273.40	0.046	13.05	100.82	11.42	0.046	556.96	0.99	Bar Fracture

Note: P_y = yield load; S_y = slip corresponding to yield; P_u = ultimate load; S_u = Slip corresponding to peak load; Δ_y = cross-head displacement at yield; Δ_u = cross-head displacement at ultimate; U_{max} = maximum bond stress; S_{max} = slip corresponding to maximum bond stress; f_{bu} = stress in bar; R_y = (Nominal) strength ratio based on grade 400 MPa; R_s = (Nominal) strength ratio based on grade 400 MPa steel.

[(1)] **NS** refers to Non Shrink grout; **6** and **12** refer to the bar embedded length, respectively; **D and S** refer to deformed steel and Smooth steel bars, respectively.

The test results of eight specimens are shown in Table 1. The yielding load, P_y, was extracted from the data with the aid of a routine written specifically to identify changes in the elastic slope of the load-displacement curve. The reported displacements, Δ_y and Δ_u, were taken as the relative movement of the fixed and moving heads of the testing machine at the yield and peak loads, respectively. At any point during the test, the slip of the bar was obtained from the measurements recorded by the upper LVDT. The stress f_{bu}, was based on actual bar diameters (490.8 mm^2). U_{max}, was calculated using Equation 2:

[2] $$U = \frac{P}{\pi d L_d}$$

Where U = bond stress; P = tensile load; d = bar diameter and L_d = embedded length in grout.

4.1. Bond Stress-Slip Behaviour

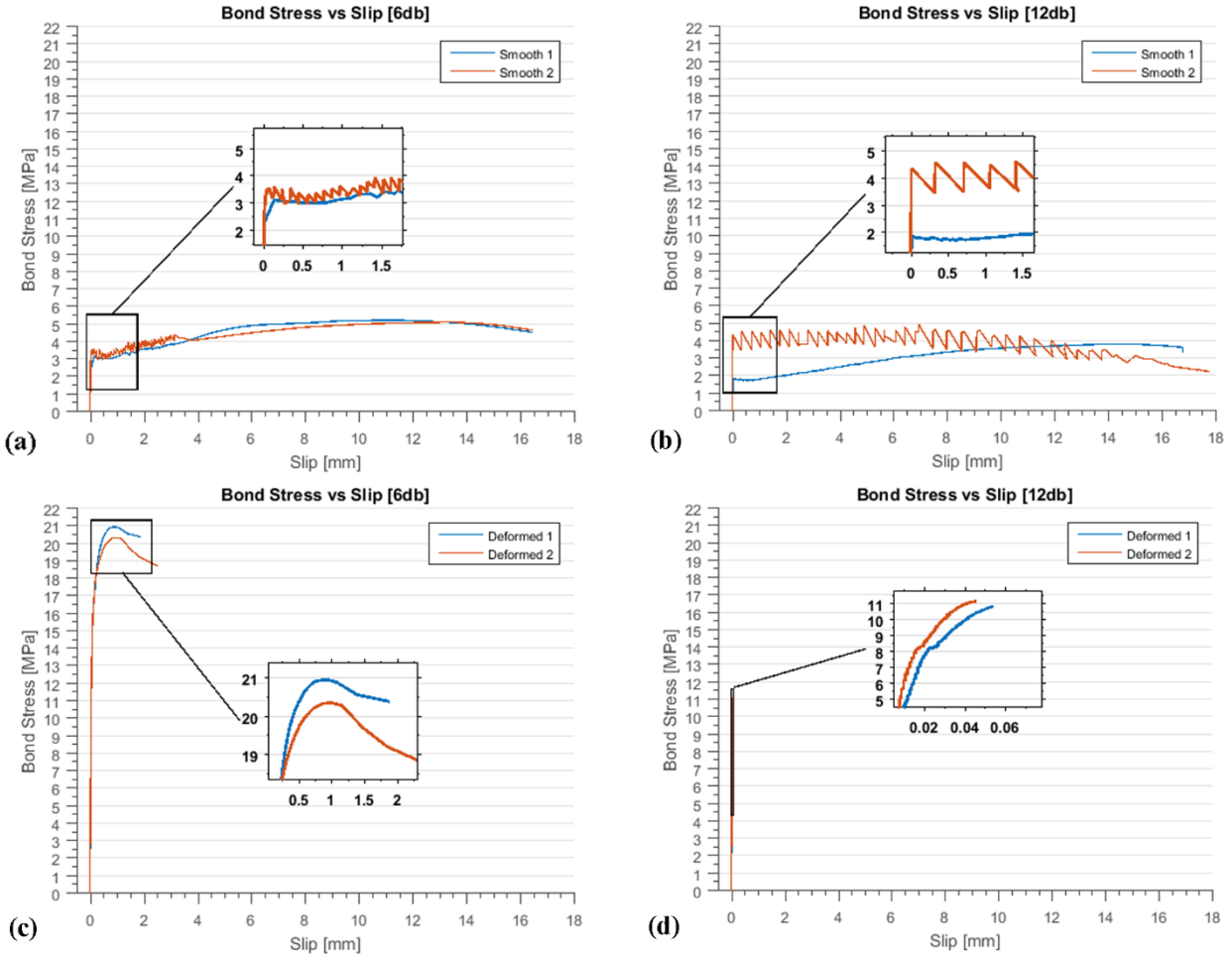

Figure 4: Comparison between bond stress-slip curves for smooth and deformed bars: (a) ld = $6d_b$ (smooth); (b) ld = $12d_b$ (smooth); (c) ld = $6d_b$ (deformed); (d) ld = $12d_b$ (deformed)

The bond-slip response of the specimens tested is depicted in Figure 4. The curves of all specimens were characterized by four zones: an ascending branch where the bond strength increases with a slow increase in slip; a yielding zone where the curve experience an abrupt change in slope accompanied by a consistent increase in slip for the same bond stress; a hardening branch where the maximum bond strength is attained; and a softening branch where a gradual drop in the bond stress is accompanied by an increase in slip. The anchorage of the smooth bars was dependent on the chemical adhesion of the grout, which is a function of the compressive strength. This can be observed by examination of the ascending branch in Figures 4(a) and 4(b). Once the stress exceeds that of the adhesion limit of the grout, significant slip occurred. At the onset of this rapid slip, dislocating lumps of grout started to engage slightly increasing the resistance to pull-out. This is observed in the fluctuations apparent in the readings (Figure 4(a) and (b)). Ultimately, the bar reaches a point where these dislocating lumps cannot initiate resistance due to the lack of embedment and the bar pulls out. The behaviour of deformed bars varied significantly with the embedment length. The bars exhibited a bond-slip response similar to the described above (characterized by the four zones), however, the slip domains were much shorter than their smooth counterparts. Figure 5 compares the slip of individual specimens to the maximum

bond stress, which clearly highlights the total slip domains from its start until the maximum bond stress is attained. From Table 1, the average slip corresponding to the maximum bond stress for the $6d_b$ and 12 d_b was 0.91 and 0.05, respectively. The specimens embedded at $12d_b$ had significantly reduced slip. This is due to more bar lugs being engaged with the grout, which increased the mechanical resistance (friction and bearing), thus increasing the resistance to slip. Figure 5 compares the maximum bond strength for the different specimens. On average, smooth bars developed 25% and 38.3% the bond strength of deformed bars for embedment lengths of 6 and $12d_b$, respectively.

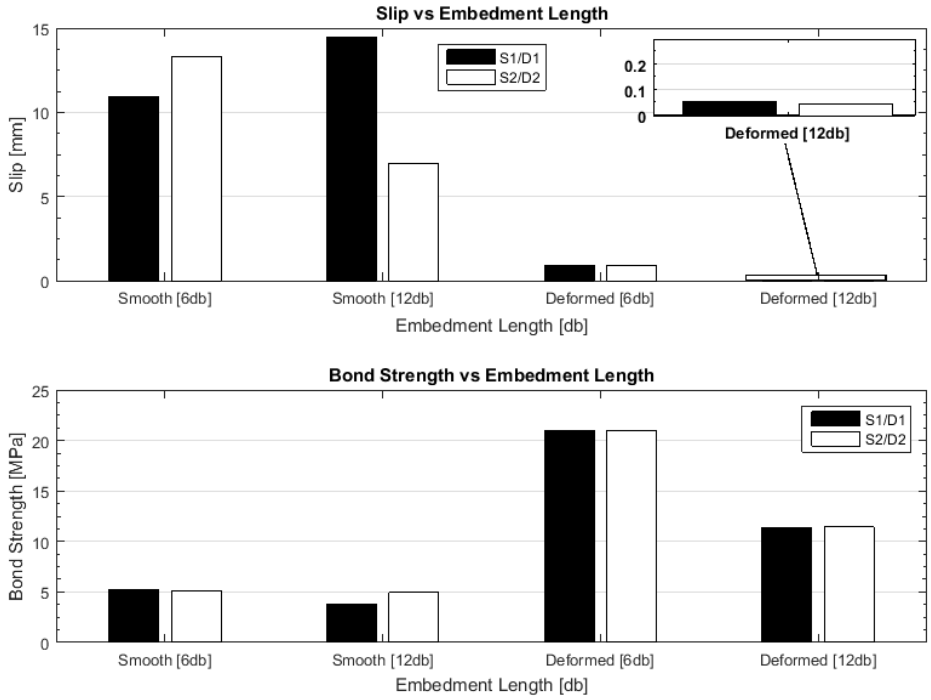

Figure 5: Comparison between bond strength and embedment length for different bars.

4.2. Failure Mode and Force-Displacement response

Failure of representative specimens of smooth and deformed bars is shown in Figure 6. The specimens were loaded uniformly using a monotonically increasing tensile load until a failure was observed. After failure, specimens were inspected visually for any cracks or deformations in the grout or the concrete. Split tensile cracks did not occur during any of the performed tests. The confinement effect of the sleeve played an important role towards this. The grout around the pulled bar dilated and expanded transversally, pushing the cover. The sleeve provided an efficient arresting mechanism to this expansion, thus eliminating this type of failure. Additionally, conical grout failures, a result of additional compression induced from the pull-out test (Steuck et al. 2009), was not observed.

Table 1 indicates that all smooth steel specimens failed by pull-out. The failure was gradual and started once the maximum bond stress was achieved. The grout at the loaded end remained intact after slippage, as shown in Figure 6(a). The failure of the deformed bar specimens, embedded at $6d_b$, is shown in Figure 6(d). The bar in the specimen yielded at a stress of approximately 400 MPa. Loading beyond the yield point resulted in a bar pull-out at the strain hardening zone. Although the bond strength was largest for the $6d_b$ specimens (~20.65 MPa), the lack of sufficient embedment length caused the pull-out failure. Deformed bars embedded $12d_b$ all failed by bar fracture, as shown in Figure 6(c). The specimen behaved similar to its $6d_b$ counterpart, up until the yielding point, after which, the bar sustained loading up to its capacity and fractured. The bond strength in the $12d_b$ specimens was approximately half of the 6db counterparts.

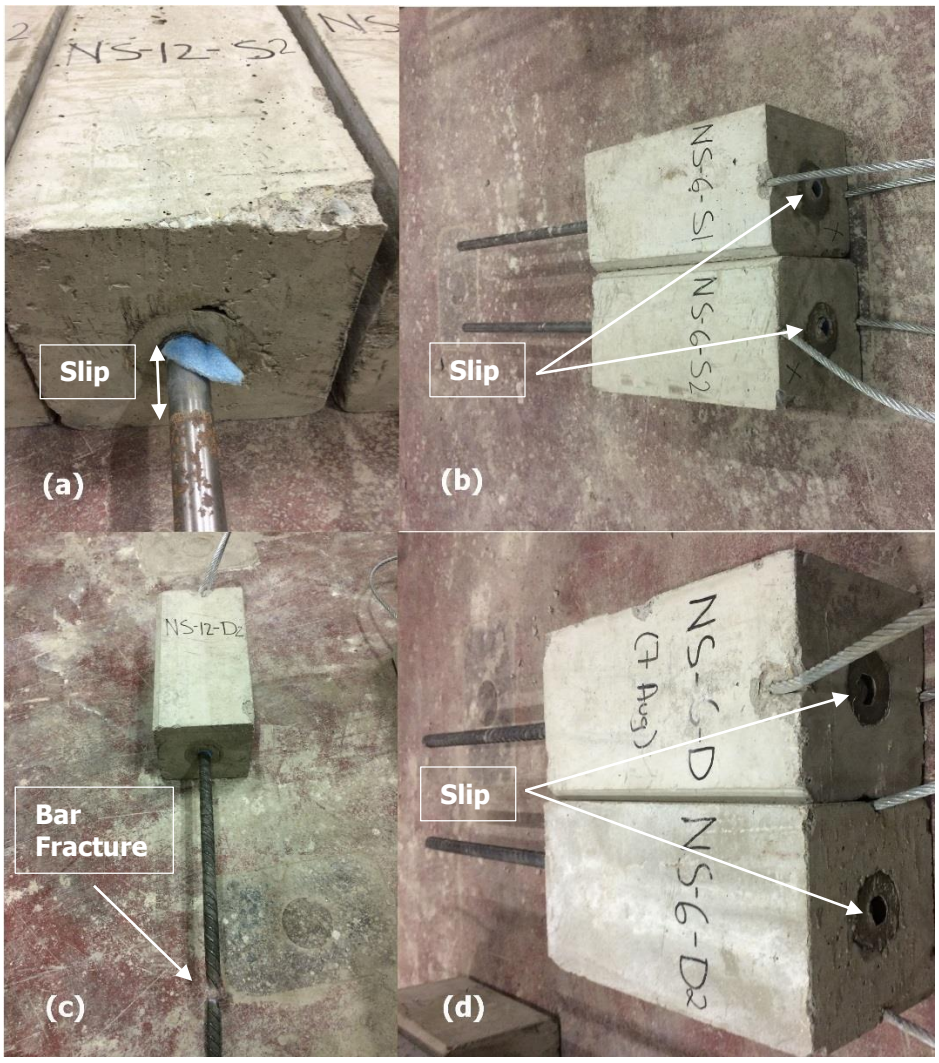

Figure 6: Specimen failure modes: (a) NS-12-S2; (b) $12d_b$ smooth specimens; (c) bar fracture in the deformed $12d_b$ specimens; (d) slippage in the NS-6-D specimens

Figure 7 compares the force-displacement curves of various specimens. The general trend follows that of a classical force-displacement coupon response. The yielding load of specimens D1 and D2 embedded at $6d_b$ and $12d_b$, was 198.0, 197.2, 197.1 and 197.4, respectively, with an average of 197.4 MPa and a standard deviation of 0.40 MPa. The $6d_b$ specimens failed by pull-out of the bars past the yielding point at 250.8 and 243.6 kN, respectively, while their $12d_b$ counterparts failed by rupture of the bar at 273.1 and 273.4 kN, respectively. To quantify the capacity of the embedment length and the over-all load carrying capacity of the connection, a ratio was devised to measure the capacity of the connection compared to that of a bar (after Ling et al. 2012). Equation 3 calculates the yield ratio as follows:

$$[3] \qquad R_y = \frac{P_y(Specimen)}{p_y(Specified)}$$

The yield ratio R_y is calculated in Table 1 for the specimens of the study. A specimen with a yield ratio of at least 1 indicates yielding of the bar and a desirable response. Smooth bars embedded $6d_b$ and 12 d_b achieved an average yield ratio of 20% and 49%, respectively. All deformed bars achieved a yield ratio of 0.99 indicating yielding of the bars.

Yielding of bars in grouted bar connections provides ductility to precast wall assemblies, which is often in the form of opening of the horizontal 1" (25.4 mm) grout bed customarily placed between stacked panels.

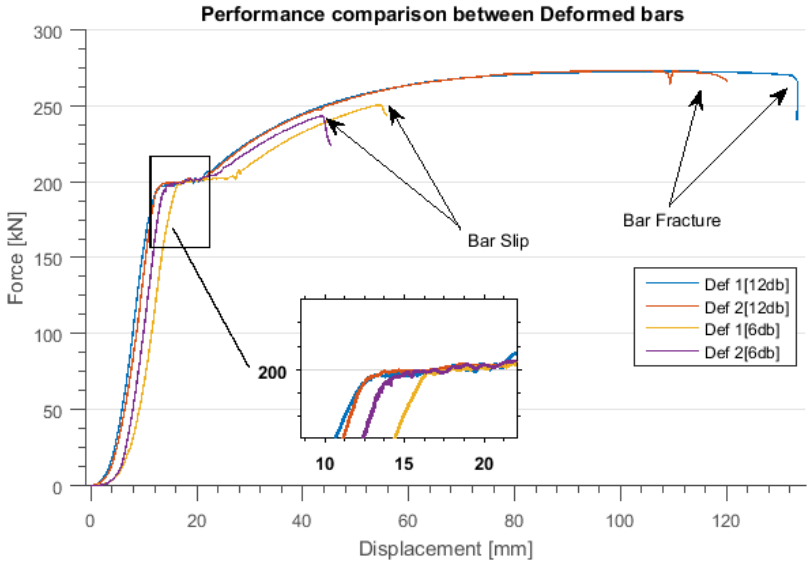

Figure 7: Force-displacement comparison between deformed bar specimens

5. CONCLUSIONS

Eight pull-out tests were conducted to study the bond and capacity of grouted bar-in-conduit connections and benchmark their pull-out resistance at shorter embedment lengths. The main test parameters were the bar surface condition (smooth and deformed) and the embedment length ($6d_b$ and $12d_b$). Bond strength, slip, displacement and load carrying capacity were extracted and compared. Based on the test results, the following concluding remarks can be drawn:

1) The behaviour of bond between reinforcing bars and grout, bound by the corrugated steel sleeve, is different than that of a classical reinforcing bar-in-concrete problem. The continuous confinement of the sleeve along the grouted length arrests the expansion of grout, limiting splitting tensile failures.
2) Under monotonic tensile loads, an embedment length of $6d_b$ was sufficient to cause the bar to yield, while a $12d_b$ embedment mobilized the tensile capacity of the bar. The behaviour of grouted sleeve connections under cyclic loading is yet to be investigated to confirm if the latter embedment length provides the adequate ductile response under reversing strain demand.
3) The adequacy of using the ACI-318-14 development length model is debatable. An empirical model capable of predicting the bond behaviour of sleeve-confined bar in grout is necessary to predict the behaviour and reduce field grouting lengths.

ACKNOWLEDGEMENTS

The authors would like to acknowledge and thank Stubbe's Precast (Brant, Ontario) for their donation of materials and other technical expertise throughout this project.

REFERENCES

Achillides, Z. & Pilakoutas, K., 2004. Bond Behavior of Fiber Reinforced Polymer Bars under Direct Pullout Conditions. *Journal of Composites for Construction*. Available at: http://ascelibrary.org/doi/10.1061/%28ASCE%291090-0268%282004%298%3A2%28173%29 [Accessed December 17, 2015].

ACI Committee 318, 2014. *ACI 318-14: Building Code Requirements for St*,

ACI Committee 408, 2003. Bond and Development of Straight Reinforcing Bars in Tension Reported by ACI Committee 408. *Aci 408-03*, pp.1–49.

CPCI, 2007. *design manual 4*,

Dancygier, A.N., Katz, A. & Wexler, U., 2010. Bond between deformed reinforcement and normal and high-strength concrete with and without fibers. *Materials and Structures*, 43(6), pp.839–856.

Fintel, M., 1977. Performance of Precast Concrete Structures during Romanian Earthquake of March 1977. *PCI Journal*, 22.

Harajli, M., Hamad, B. & Karam, K., 2002. Bond-slip Response of Reinforcing Bars Embedded in Plain and Fiber Concrete. *Journal of Materials in Civil Engineering*, 14(6), pp.503–511.

Hosseini, S.J.A. et al., 2015. Bond behavior of spirally confined splice of deformed bars in grout. *Construction and Building Materials*, 80, pp.180–194. Available at: http://linkinghub.elsevier.com/retrieve/pii/S0950061814013993.

Ling, J.H. et al., 2012. Behaviour of grouted pipe splice under incremental tensile load. *Construction and Building Materials*, 33, pp.90–98. Available at: http://dx.doi.org/10.1016/j.conbuildmat.2012.02.001.

Ling, J.H., Ahmad, A.B. & Ibrahim, I.S., 2014. Feasibility study of grouted splice connector under tensile load. *Construction and Building Materials*, 50, pp.530–539. Available at: http://dx.doi.org/10.1016/j.conbuildmat.2013.10.010.

PCI, 2010. *PCI DESIGN HANDBOOK 7th edition*,

Raynor, D.J., Dawn, E.L. & Stanton, J.F., 2002. Bond-Slip Response of Reinforcing Bars Grouted in Ducts. *ACI Structural Journal*, 99(5), pp.568–576.

Saleem, M.A. et al., 2012. Development Length of High-Strength Steel Rebars in Ultra-High Performance Concrete. *Journal of Materials in Civil Engineering*, (August), p.120827055859009.

Soroushian, P. et al., 1991. Bond of deformed bars to concrete: effects of confinement and strength of concrete. *ACI Materials Journal*. Available at: http://www.concrete.org/publications/internationalconcreteabstractsportal.aspx?m=details&i=1818 [Accessed November 23, 2015].

Steuck, K.P., Eberhard, M.O. & Stanton, J.F., 2009. Anchorage of large-diameter reinforcing bars in ducts. *ACI Structural Journal*, 106(106), pp.506–513.

Tastani, S.P. & Pantazopoulou, S.J., 2010. Direct Tension Pullout Bond Test: Experimental Results. *Journal of Structural Engineering*, 136(6), pp.731–743.